Catalysis Today 138 (2008) 21–27

Contents lists available at ScienceDirect

Catalysis Today

journal homepage: www.elsevier.com/locate/cattod

Comparative study of H_2 production by ethanol steam reforming on $Ce_2Zr_{1.5}Co_{0.5}O_{8-\delta}$ and $Ce_2Zr_{1.5}Co_{0.47}Rh_{0.07}O_{8-\delta}$: Evidence of the Rh role on the deactivation process

Mirella Virginie [a], Marcia Araque [a,b], Anne-Cécile Roger [a,*], Julio César Vargas [b], Alain Kiennemann [a]

[a] Laboratoire des Matériaux, Surfaces et Procédés pour la Catalyse LMSPC, UMR CNRS 7515, ECPM - Université Louis Pasteur, 25 rue Becquerel, 67087 Strasbourg Cedex 2, France
[b] Departamento de Ingeniería Química y Ambiental, Universidad Nacional de Colombia Ciudad Universitaria, Avenida Carrera 30 N° 45-03, Edificio 453, Bogotá D.C., Colombia

ARTICLE INFO

Article history:
Available online 20 June 2008

Keywords:
Ethanol steam reforming
Hydrogen
Fluorite
Cobalt
Rhodium
Carbonates species

ABSTRACT

The catalytic performance of $Ce_2Zr_{1.5}Co_{0.5}O_{8-\delta}$ and $Ce_2Zr_{1.5}Co_{0.47}Rh_{0.07}O_{8-\delta}$ mixed oxides was evaluated comparing the influence of Rh insertion for hydrogen production in ethanol steam reforming. Rh doped and not doped catalysts were prepared by the pseudo sol–gel like method and were characterized using DRX, TPR, SEM, and TPO. For the Rh-doped catalyst, it was found an easier structure reducibility allowing to avoid a reducing activation treatment. The reactivity results show that lifetime of $Ce_2Zr_{1.5}Co_{0.47}Rh_{0.07}O_{8-\delta}$ mixed oxide is more than 30 times higher, compared to the $Ce_2Zr_{1.5}Co_{0.5}O_{8-\delta}$ mixed oxide. Catalytic tests under various water/ethanol ratios and ethylene and acetaldehyde steam reforming evidence that the deactivation process for the catalytic systems is not only related to carbon deposits but also to carbonate species, which can be form from an acetaldehyde reaction sequence. The benefic effect of rhodium would ascribe to its ability to avoid carbonates formation under reaction, preventing the blocking of the active oxygen vacancies of the mixed oxide support.

1. Introduction

The increase of greenhouse gases in the atmosphere, particularly CO_2, which strictly arises from the use of fossil fuels, has led to the search of alternative energy sources. Hydrogen represents a non-polluting fuel, clean energy, which is efficient, economically attractive and non-associated with polluting gases emissions [1]. It can be produced from several sources; nevertheless, the main ones are non-renewable implying that the transformation processes involve the formation of CO_2 as a by-product. The hydrogen production from bioethanol seems to be an alternative to this problem. Bioethanol can be obtained in large quantities, like a renewable energy source, by fermentation of vegetal biomass [2], and it has the advantage that the amount of CO_2 produced during fermentation and steam reforming can be considered equivalent to the amount of CO_2 consumed by the biomass during the photosynthesis process. This means that there will be no additional contribution to the greenhouse.

Ethanol steam reforming has been studied over noble metal [3–7] and transition metals [8–12] supported on a wide range of oxides with different acid–base and redox properties. The main problem for most of these systems is the high deactivation rate related with the formation of carbonaceous deposits, as a consequence of the increase in the active phase particle size by sintering.

Integration of the active phase in a support, of high oxygen mobility, has been proposed as a solution to reduce the sintering effect [13,14]. The integration enhances the metal/support interaction and consequently diminishes the carbonaceous deposits formation. These studies use a catalyst based on mixed oxides, a fluorite-type structure CeZrCo, which active phase (Co) has been initially integrated to the support structure. These oxides have already shown high activity, selectivity and catalytic stability for the ethanol steam reforming [13,14]. However, after a few hours of total conversion, the formation of by-products as ethylene, acetaldehyde and acetone is often observed, which greatly affects the activity and stability of the catalyst and leads to the deactivation. After test, carbonaceous deposits were observed at the catalyst surface and they have been correlated with the deactivation phenomena [15,16].

The influence of the active phase modification (Co, Ni, Rh) on the catalytic behavior, was evaluated on previous studies [17,18], concluding that addition of small amounts of a noble metal as Rh improves the catalytic performance and reduce the formation of

* Corresponding author. Fax: +33-390242768.
E-mail address: rogerac@ecpm.u-strasbg.fr (A.-C. Roger).

0920-5861/$ – see front matter © 2008 Elsevier B.V. All rights reserved.
doi:10.1016/j.cattod.2008.04.047

carbonaceous deposits limiting as well the formation of by-products.

This work compares the catalytic performance of the mixed oxides $Ce_2Zr_{1.5}Co_{0.5}O_{8-\delta}$ (named CeZrCo) and $Ce_2Zr_{1.5}Co_{0.47}Rh_{0.07}O_{8-\delta}$ (named CeZrCoRh) in ethanol steam reforming. The effect of the noble metal inclusion was analyzed on the reactivity system, the deactivation process and the catalytic behavior. The conditions of catalyst deactivation were studied varying the conditions of the ethanol steam reforming system from a mixture less reducing to a mixture more reducing, changing the feed molar ratio ethanol/water

During the steam reforming, the ethanol decomposes by two ways producing two different intermediates: ethylene by dehydration and acetaldehyde by dehydrogenation. Reforming these species can help to understand the catalysts behavior during the ethanol steam reforming and the conditions which promote the carbonaceous species formation and the posterior deactivation.

2. Experimental

2.1. Preparattion and characterization of the catalysts

The catalysts were prepared by the pseudo sol–gel like method based on the thermal decomposition of metallic propionates [13,14,17]. In previous works, the catalyst was calcinated at 500 °C (S_{BET} = 72 $m^2\ g^{-1}$), for instance in this study the calcination temperature was increased to 700 °C ($CeZrCo_{BET}$ = 9.4 $m^2\ g^{-1}$, $CeZrCoRh_{BET}$ = 8 $m^2\ g^{-1}$), in order to improve the structure stability in the activation treatment and at the reactivity system conditions.

The mixed oxides structure was studied by X-ray diffraction in a Brucker AXS-D8 Advanced equipment, Cu Kα radiation, in an interval from $2\theta = 10^\circ$ to $2\theta = 90^\circ$.

The reducibility studies were carried out by thermoprogrammed reduction (TPR) of 0.05 g of mixed oxide, in a hydrogen flow of 3.85% diluted in argon (total flow = 52 mL min^{-1}), using a temperature ramp of 15 °C min^{-1} from room temperature to 900 °C.

The analysis of the carbonaceous deposits formed during the ethanol reforming reaction, was carried out by thermoprogrammed oxidation (TPO) of 0.05 g of catalyst after test, in a 10% of oxygen flow diluted in helium (total flow of 50 mL min^{-1}). The temperature was increased at 15 °C min^{-1} from room temperature to 900 °C. The oxidation gases were followed by mass spectrometry. The calibration of the system was based on mass 44 (corresponding to CO_2). The procedure followed for the thermoprogrammed desorption (TPD) test was similar, using a flow of 50 mL min^{-1} of pure helium. The temperature was increased at 10 °C min^{-1} from room temperature to 800 °C.

The surface morphology after test was studied by Scanning Electron Microscopy on a JEOL JSM-6700F apparatus.

2.2. Catalytic tests

The ethanol steam reforming was carried out in a fixed bed reactor at atmospheric pressure. The CeZrCo oxide was reduced before the reaction test: the sample (0.16 g) was submitted in a 3 mL min^{-1} flow of pure hydrogen from room temperature to 440 °C (2 °C min^{-1}). These conditions were maintained during 12 h. The hydrogen remained into the reactor was eliminated by passing through an argon/nitrogen mixture (total flow of 2.1 L h^{-1}, 4/1 M). Finally, the ethanol/water mixture (0.9 L h^{-1} of mixture in gas phase for ethanol/water = 1/6) was introduced into the reactor which was previously heated at 550 °C. The space velocity (GHSV) was 26,000 h^{-1} for the tests over the $Ce_2Zr_{1.5}Co_{0.5}O_{8-\delta}$ oxide and for the stability ethanol reforming test over the $Ce_2Zr_{1.5}Co_{0.47}Rh_{0.07}O_{8-\delta}$. This value was increased to 41,000 h^{-1} for the Rh-doped catalyst in the comparative analysis between ethylene, acetaldehyde and ethanol steam reforming. The feed molar ratio used was 1/6 in the ethanol stability steam reforming and ethylene and acetaldehyde reforming reaction.

The influence of the redox atmosphere in the deactivation process was evaluated using three ethanol/water molar ratios: 1/3, 1/4.5 and 1/6. The GHSV and the amount of ethanol per gram of catalyst were maintained constant during the reaction, changing the mass of the catalyst in the reactor and the flow of argon/nitrogen mixture: 0.190 g and 2.8 L h^{-1} for the 1/4.5 ratio, and 0.238 g and 3.7 L h^{-1} for the ratio 1/3, measured at STP conditions.

The effluent compounds were analyzed on line by gas microchromatograph (Poraplot Q and molecular sieve 5 Å columns).

3. Results and discussion

3.1. Characterization before catalytic test

The mixed oxide diffractograms before test are presented in Fig. 1. The cubic structure of $Ce_2Zr_2O_8$ is clearly evidenced; nevertheless it is observed for the $Ce_2Zr_{1.5}Co_{0.5}O_{8-\delta}$ and the $Ce_2Zr_{1.5}Co_{0.47}Rh_{0.07}O_{8-\delta}$ oxides a small diffraction peak (36.8°), attributed to Co_3O_4 spinel phase, indicating a small rejection. This phenomenon was not observed when the calcination temperature was 500 °C [13]. No Rh_2O_3 characteristic peaks were found in the CeZrCoRh oxide. The cubic lattice parameters of the cubic face centered fluorite were 5.30 Å for the CeZrCo and 5.28 Å for the CeZrCoRh oxide. They were calculated from the five most intense diffraction peaks [1 1 1], [2 0 0], [2 2 0], [3 1 1] and [2 2 2].

TPR profiles are given in Fig. 2. It is observed that the Co insertion in the oxide solid solution clearly modifies the CeZr reduction profile, lowering the maximum temperature of the first reduction zone from 588 to 421 °C. This effect is stronger when Rh is added into the oxide, where the first reduction peak appears at 243 °C. For the second reduction zone, the general behavior was similar: the peak temperature decreased from 900 to 705 °C with the Co insertion and it reached a value of 670 °C with the rhodium presence. It can be noted a shoulder at 301 °C for CeZrCoRh and at 353 °C for CeZrCo which could correspond to the hydrogen consumption by the rhodium or cobalt reduction which are differently linked to the structure. The H_2 consumption was 1.7 mmol $H_2\ g_{cat}^{-1}$ for the CeZr; 3.07 mmol $H_2\ g_{cat}^{-1}$ for the CeZrCo; and 3.14 mmol $H_2\ g_{cat}^{-1}$ for the CeZrCoRh oxide. These values indicate that the reduction of cerium IV into cerium III was complete for the three catalysts, and also that there was a total cobalt and rhodium reduction into metals (Co^{3+} into Co^0 and Rh^{3+}

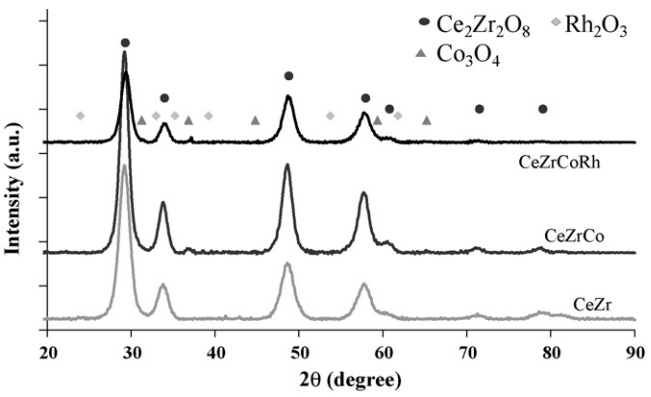

Fig. 1. Diffractograms of fresh mixed oxides CeZr, CeZrCo and CeZrCoRh.

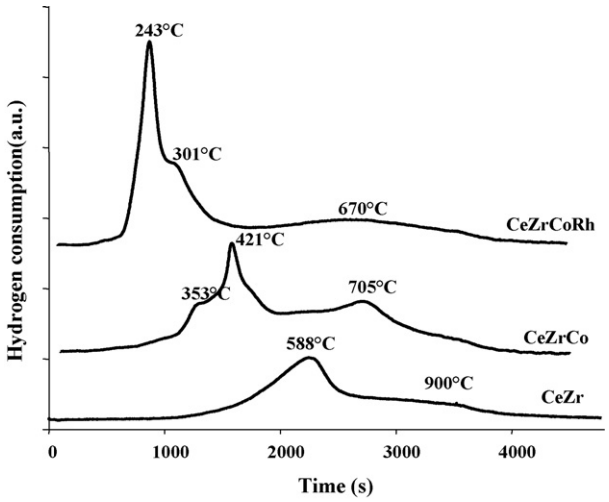

Fig. 2. Thermograms of hydrogen consumption in thermoprogrammed reduction of mixed oxides CeZr, CeZrCo and CeZrCoRh.

into Rh^0). Consequently, cobalt and rhodium insertion in the lattice affect more the reduction temperature than the reducibility of the CeZr fluorite [18,19].

3.2. Preliminary catalytic tests

The effect of the reduction state on the catalytic activity was preliminary evaluated by performing different activation procedures. The ethanol reforming was carried out over the CeZrCo oxide: (a) without any reduction treatment, (b) after a partial reduction treatment at 450 °C and (c) after total reduction at 750 °C. In Fig. 3 the H_2 yields obtained for each case are presented and they are compared with the ones obtained by the thermodynamic calculations.

The hydrogen production for the CeZrCo oxide is very low when it is used without any treatment (0.1 g H_2 g_{cat}^{-1} h^{-1} at 550 °C (Fig. 3a)). This value slightly increased to 0.19 g H_2 g_{cat}^{-1} h^{-1} at 550 °C (Fig. 3c), when the catalyst is completely reduced, and it reaches the best productivity when is partially reduced at 450 °C (0.3 g H_2 g_{cat}^{-1} h^{-1}, at 550 °C). These results indicate that the reduction state strongly affects the $Ce_2Zr_{1.5}Co_{0.5}O_{8-\delta}$ catalytic activity, presenting an optimal performance when there is the presence of both metallic and oxidized phases.

The CeZrCoRh hydrogen production is higher than that for the CeZrCo oxide, at all the temperatures. The H_2 production reaches the expected thermodynamic value (0.38 g H_2 g_{cat}^{-1} h^{-1} at 550 °C), with or without any preliminary reduction treatment, demonstrating that initial reduction is not necessary to exhibit high activity when Rh is present even in low amount. The easier reducibility of the system induced by the presence of Rh, highlighted by the TPR results (main reduction at 243 °C under H_2), allows to reduce the CeZrCoRh under reaction conditions (1/6 ethanol/water mixture at 550 °C).

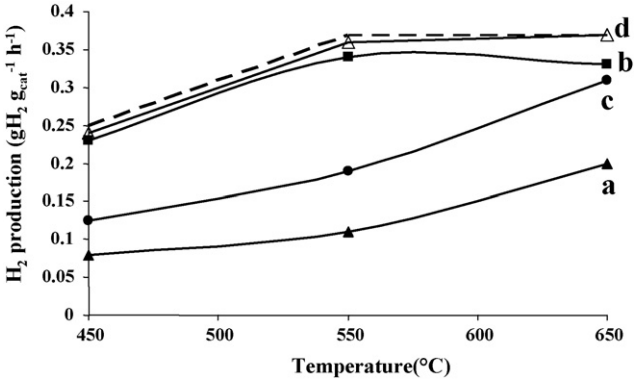

Fig. 3. Hydrogen production (g H_2 g_{cat}^{-1} h^{-1}) at different temperatures of ethanol reforming (ethanol/water = 1/6). (a) CeZrCo without any reduction, (b) CeZrCo after partial reduction, (c) CeZrCo after total reduction, and (d) CeZrCoRh without any reduction and (- - -) thermodynamic curve.

3.3. Isothermal ethanol reforming (1/6 ethanol/water mixture)

The CeZrCo and the CeZrCoRh catalysts were comparatively tested under isothermal conditions (550 °C), to study the influence of Rh insertion on the system stability (lifetime and deactivation behavior). The CeZrCo catalyst was activated under H_2 at 450 °C to ensure maximal activity, while for the CeZrCoRh no activation treatment was performed. The results are presented in Fig. 4.

For the two systems, complete ethanol conversion was achieved during the first hours. The main products gas distribution is similar for both oxides: around 65% of H_2, 25% of CO_2 and 8% of CO. For the $Ce_2Zr_{1.5}Co_{0.5}O_{8-\delta}$ catalyst, the deactivation begins after 5 h of reaction, reaching a 60% conversion after 25 h (Fig. 4a). For the $Ce_2Zr_{1.5}Co_{0.47}Rh_{0.07}O_{8-\delta}$ oxide, the decrease of ethanol conversion begins only after 150 h, and after 250 h of reaction it still remains over 70% (Fig. 4b).

The by-products selectivity is presented in Fig. 5a for CeZrCo and in Fig. 5b for CeZrCoRh. It is observed for the CeZrCo catalyst, that the deactivation phenomenon is accompanied by a slightly decrease of CO selectivity, a major increase in acetaldehyde production (from 0 to 6%), and a maximum in ethylene (0.8%) and acetone (1.5%) formation. The methane selectivity remains almost constant at 1% during the whole reaction time.

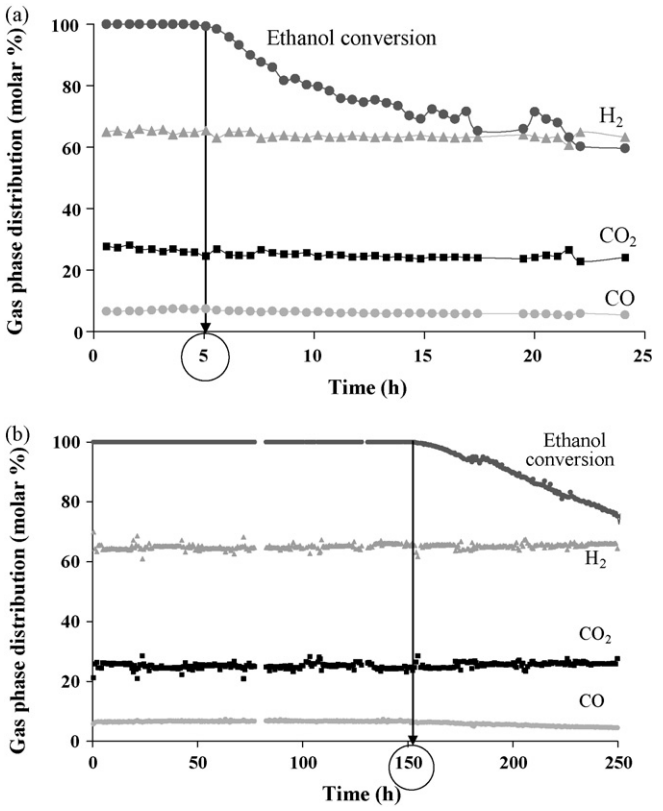

Fig. 4. Ethanol conversion and molar distribution (%) of H_2, CO_2 and CO in the gas phase of (a) CeZrCo catalyst and (b) CeZrCoRh catalyst. Reaction at 550 °C, ethanol/water 1/6.

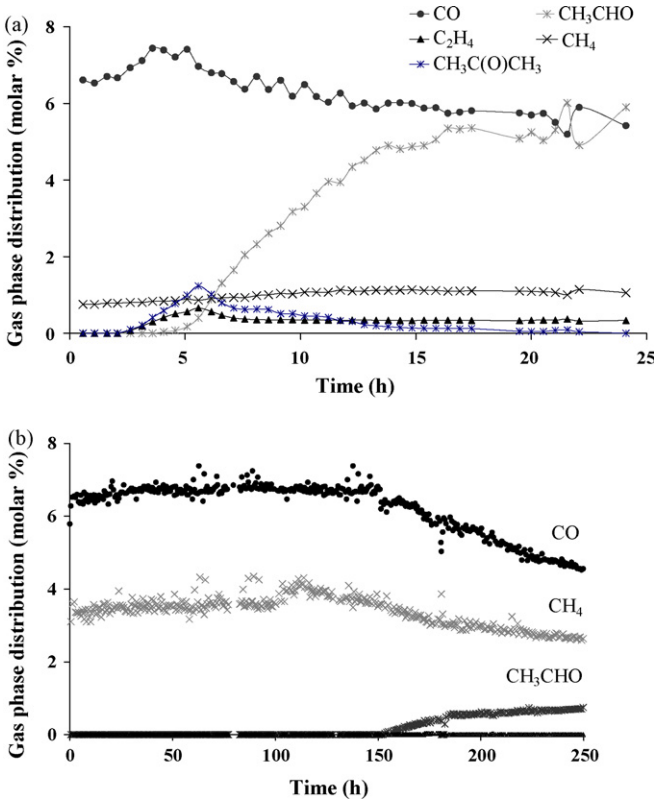

Fig. 5. Molar distribution (%) of CH_4, CO, C_2H_4, CH_3CHO, and CH_3COCH_3 in gas phase of (a) CeZrCo catalyst and (b) CeZrCoRh catalyst. Reaction at 550 °C, ethanol/water 1/6.

For the CeZrCoRh oxide, the gas phase distribution is different (Fig. 5b), remarking the absence of ethylene and acetone as by-products. When the deactivation process begins in this system (150 h), it is also observed a drop in the CO production (6–4% gas phase) and the presence and increment of acetaldehyde in gas phase. The behavior observed for the CH_4 is similar to that presented for the CO. It must be noticed that methane is produced in a higher extent (~4%) compared to the catalyst free of Rh (<1%).

After test, the two catalysts were characterized by thermo-programmed oxidation (Fig. 6). The TPO profiles are similar, showing two different oxidation zones: the first one at low temperature (around 300 °C) and the second one at a temperature around 500 °C, which is generally ascribed to carbon deposits oxidation [17].

The global CO_2 production for the CeZrCo catalyst is 5.7 mmol CO_2 g_{cat}^{-1}, while for the CeZrCoRh is 7.7 mmol CO_2 g_{cat}^{-1}. 1. Nevertheless, it must be pointed out that even the overall CO_2 production for the CeZrCo catalyst is lower than the one for the Rh catalyst, this value must be related with the amount of carbon converted during the steam reforming test, which is approximately 16.9 mol for CeZrCoRh and 1.2 mol for CeZrCo.

The relative intensity of the two peaks is very different as it is the amount of CO_2 produced at each zone. For the $Ce_2Zr_{1.5}Co_{0.5}O_{8-\delta}$, the first oxidation peak (300 °C) has a higher intensity than that exhibited for the catalyst with Rh. This zone represents the 41% of the total CO_2 production (2.3 mmol CO_2 g_{cat}^{-1}), while for the CeZrCoRh catalyst it is only the 21% of the total CO_2 formed (1.6 mmol CO_2 g_{cat}^{-1}). From TPO tests, it seems that deactivation is directly related to species which oxidize into CO_2 at low temperature.

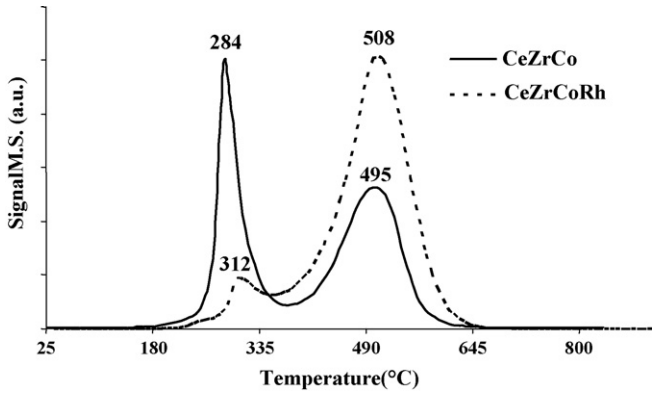

Fig. 6. TPO profiles of CeZrCo catalyst after 25 h and CeZrCoRh catalyst after 350 h of reforming. Reaction at 550 °C, ethanol/water 1/6.

3.4. Isothermal ethanol reforming (different ethanol /water ratios)

Catalytic tests under different ethanol/water ratios (1/6; 1/4.5 and 1/3) were performed, in order to study the influence of the redox atmosphere on the carbon deposits and the deactivation phenomenon. The test was carried out over the $Ce_2Zr_{1.5}Co_{0.5}O_{8-\delta}$ oxide keeping constant the amount of ethanol per hour per mass of catalyst introduced into the reactor. The ethanol conversion is presented in Fig. 7.

As expected, the system stability increased as the ethanol/water ratio decreases. While deactivation occurred immediately for the 1/3 mixture, it was observed after 2 h for the 1/4.5 mixture and after 5 h for the 1/6 one, meaning that the deactivation process is enhanced by the reducing capacity of the reactant mixture.

TPO after test (Fig. 8) shows a relationship between the deactivation time and the intensity of the first oxidation peak. It can be seen that the structure less stable is the one who has the highest intensity peak (mixture 1/3), while the lowest intensity for this signal is for the 1/6 test (more stable). The second peak of oxidation (480 °C) is generally ascribed to filamentous carbon [17], in this case related to the amount of reacted ethanol.

Catalyst SEM observations after tests are shown in Fig. 9. The most stable system (1/6 mixture), the one that transformed more ethanol, is almost completely covered by carbon filaments (Fig. 9a), while the catalyst for mixture 1/3 is almost free of them (Fig. 9c). Thus, in agreement with TPO results, carbon filaments are not directly related to deactivation. This is a clear indication that in ethanol reforming over a ceria-zirconia catalyst filamentous carbon is not directly related to deactivation, which is not in accordance with the results generally obtained in methane steam reforming.

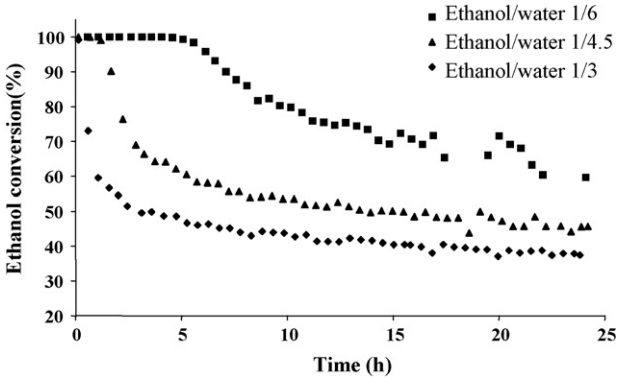

Fig. 7. Ethanol conversion (%) for various molar ratios of ethanol/water over CeZrCo.

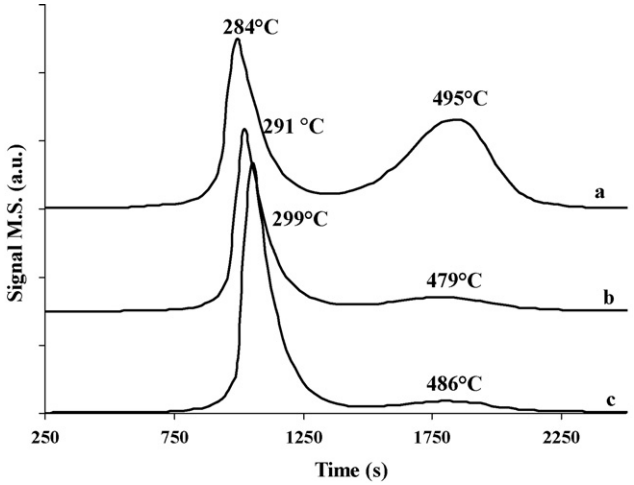

Fig. 8. TPO profiles of the CeZrCo catalyst after test at 550 °C at various ethanol/water ratios: (a) 1/6, (b) 1/4.5 and (c) 1/3.

3.5. Isothermal acetaldehyde and ethylene reforming

Ethanol activation follows two major sequences depending on the catalyst properties: dehydrated into ethylene (C_2H_4) over the acid sites or dehydrogenated into acetaldehyde (CH_3CHO) over the basic sites or redox sites [20]. A way to recognize the most favorable mechanism is to evaluate if the catalyst is able to reform these intermediates and how well it does it.

Acetaldehyde and ethylene steam reforming have been performed at 550 °C with a ratio reactant/water of 1/6. For the CeZrCo oxide it was used a GHSV of 26,000 h^{-1} while for the CeZrCoRh this value was increased to 41,000 h^{-1} to accelerate the deactivation process. The reaction was followed during 25 h.

The hydrogen production and the reactant conversion were calculated for each test (Fig. 10). The different curves show that for all the reactants (ethanol, acetaldehyde and ethylene), the Rh catalyst is more active and more H_2 selective than the catalyst with only Co. For ethanol reforming, the hydrogen production is quite stable for the CeZrCoRh catalyst (0.55 g H_2 g_{cat}^{-1} h^{-1}), while it decreases from 0.38 to 0.20 g H_2 g_{cat}^{-1} h^{-1} for the CeZrCo. In ethylene reforming H_2 production was stable during the 25 h of reforming: around 0.45 g H_2 g_{cat}^{-1} h^{-1} for CeZrCoRh and 0.27 g H_2 g_{cat}^{-1} h^{-1} for CeZrCo. Finally the highest deactivation was obtained for the acetaldehyde reforming, where this value decreases for the two catalysts: from 0.65 to 0.20 g H_2 g_{cat}^{-1} h^{-1} with CeZrCoRh and from 0.30 to 0.10 g H_2 g_{cat}^{-1} h^{-1} with CeZrCo. It seems that both catalysts are able to transform acetaldehyde (conversion within the range 100–70%), but they form preferably CH_4 compared to the ethylene steam reforming, diminishing the H_2 produced (Table 1).

TPO after test (Fig. 11) shows the formation of the same carbon deposits for the three reactants steam reforming: one between 200 and 400 °C, and another between 400 and 600 °C. Nevertheless, the proportion among the different curves changes depending on the reactant and the catalyst involved. For the CeZrCo catalyst, the CO_2 signal is more intense at low temperature for the ethanol and acetaldehyde tests while for the catalyst used at the ethylene reforming the behavior is the opposite. For the CeZrCoRh, it is the ethanol and the ethylene curves which have similar proportions (signal more intense at high temperature), while the acetaldehyde curve keeps its higher intensity at 300 °C. It seems that the first oxidation peak can be ascribed to species which are formed over the surface from an acetaldehyde decomposition sequence since they are not seen on the catalysts used for ethylene reforming. The

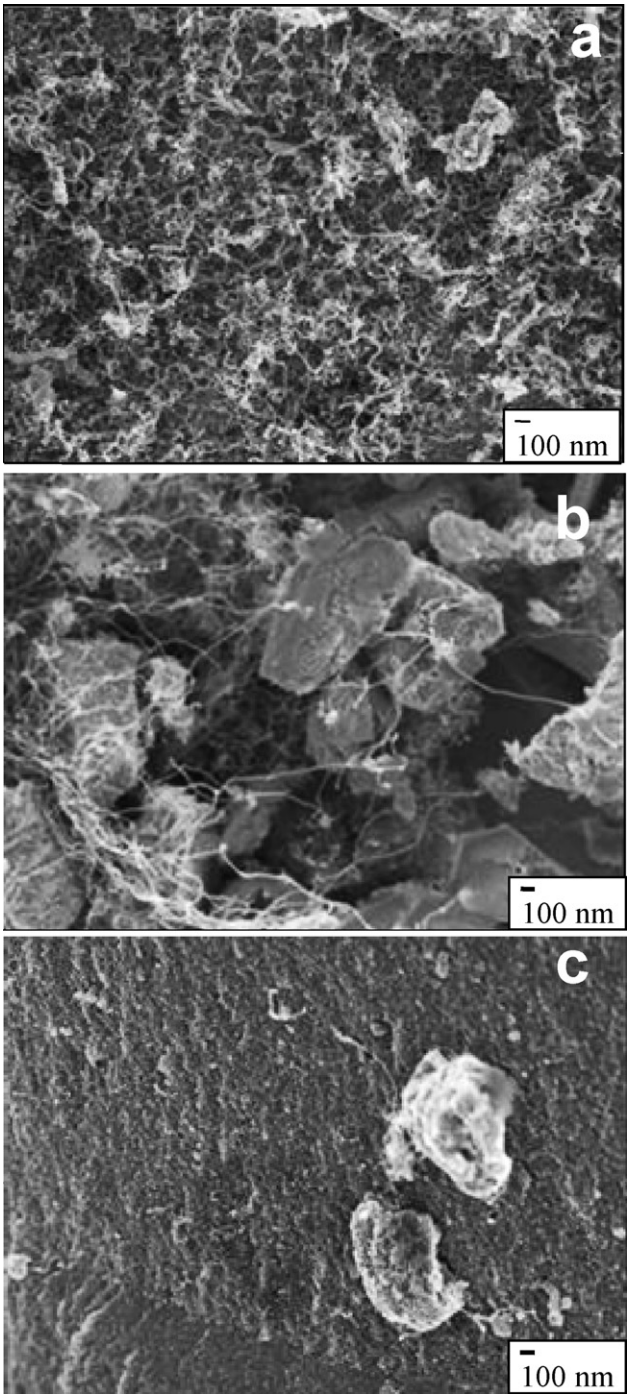

Fig. 9. SEM micrographs of the CeZrCo catalyst after test at 550 °C at different ethanol/water ratios: (a) 1/6, (b) 1/4.5 and (c) 1/3.

Table 1
Production of H_2, CO and CH_4 ($g_{compound}$ g_{cat}^{-1} h^{-1}) for the ethanol, ethylene and acetaldehyde steam reforming over the $Ce_2Zr_{1.5}Co_{0.5}O_{8-\delta}$ and $Ce_2Zr_{1.5}Co_{0.47}Rh_{0.07}O_{8-\delta}$ oxides, after 25 h of reaction

Reactive	$Ce_2Zr_{1.5}Co_{0.5}O_{8-\delta}$			$Ce_2Zr_{1.5}Co_{0.47}Rh_{0.07}O_{8-\delta}$		
	H_2	CO	CH_4	H_2	CO	CH_4
Ethanol	0.25	0.36	0.03	0.53	0.70	0.24
Ethylene	0.22	0.28	0.003	0.42	0.87	0.03
Acetaldehyde	0.13	0.20	0.02	0.32	0.50	0.11

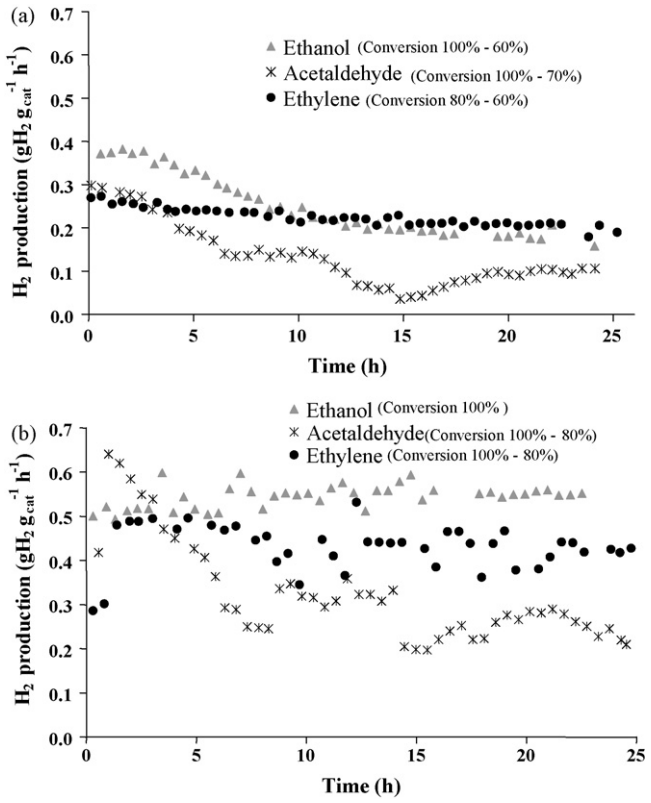

Fig. 10. Hydrogen production ($g\,H_2\,g_{cat}^{-1}\,h^{-1}$) for ethanol, acetaldehyde and ethylene reforming with (a) CeZrCo catalyst and (b) CeZrCoRh catalyst, at 550 °C during 25 h.

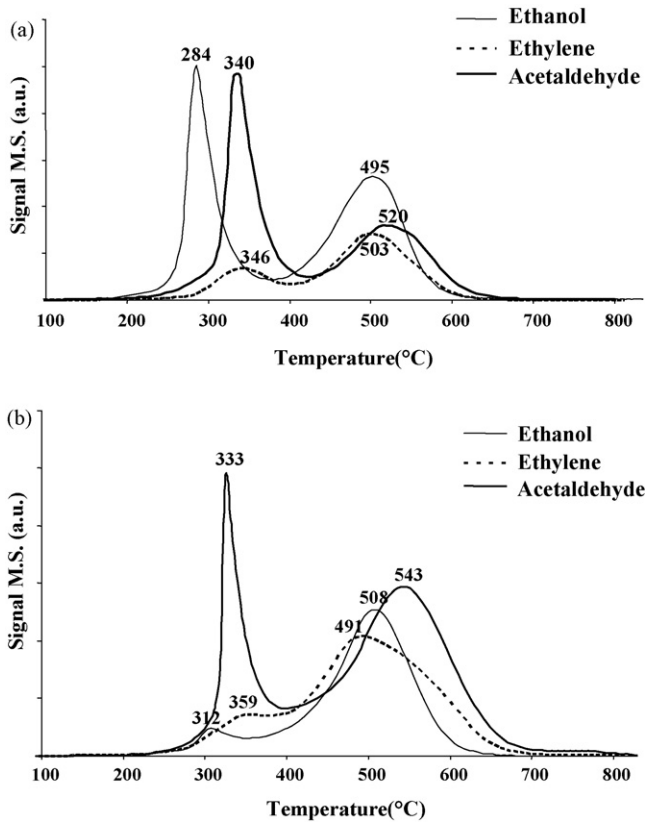

Fig. 11. TPO profiles after reforming at 550 °C of (—) ethanol, (- - -) ethylene and (▬▬) acetaldehyde over (a) CeZrCo and (b) CeZrCoRh.

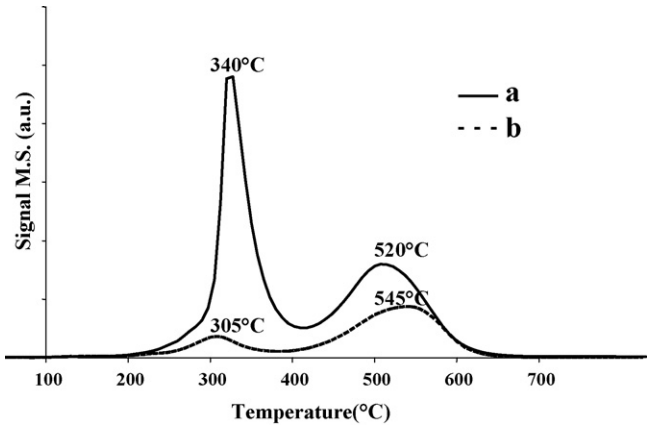

Fig. 12. TPO profiles of CeZrCo catalyst after acetaldehyde reforming (a) directly after test and (b) after TPD.

main difference arising from the presence of rhodium is that ethanol activation does not generate low oxidation temperature species, meaning that ethanol activation for the CeZrCoRh proceeds preferably through ethylene instead of acetaldehyde.

A TPD under helium was performed before the TPO measurements, for the CeZrCo oxide after acetaldehyde reforming. Desorption of the surface under inert gas leads to almost disappearance of the first TPO peak, while for the second one the effect was not so strong (Fig. 12b compare to Fig. 12a). The species arising from acetaldehyde decomposition on the surface and leading to a rapid deactivation of CeZrCo are then probably carbonate species. This is consistent with what was observed during the reactivity test with the decrease of the hydrogen production despite the high percentage of acetaldehyde conversion. The catalysts convert acetaldehyde but produce carbonates species on their surface which causes a decline of the hydrogen productivity. These carbonate species have been evidenced by "in operando" IR over CeZrCo catalysts [21].

4. Discussion

Several studies have proved that ethanol adsorbs over metal oxide catalyst as ethoxy species, by the dissociation of the O–H bond [22]. This ethoxy specie undergoes to acetaldehyde by dehydrogenation and produce hydrogen, helped by the hydroxyl groups formed on the metal surface. Acetaldehyde is then adsorbed, generating surface acetate species, which can produce acetone by the union of two of them or can lead to carbonate species by dissociation [23,24]. This mechanism is in agreement with the species observed as by-product during the ethanol steam reforming: acetaldehyde and acetone for the CeZrCo oxide.

TPO profiles have shown that the deactivation process has a strong relationship with the first oxidation peak, while the second one is more related to the amount of transformed reactant. Moreover, for the two catalysts, it can be seen that the first oxidation peak can be attributed to carbonate species generated by acetaldehyde oxidation. As it is known, the fluorite structure has a high oxygen mobility and storage capacity, being able to reduce and oxidize itself rapidly under redox conditions. When acetate and then carbonates species are formed on the catalytic surface, the structure oxygen is mobilized; thus, the formation of these species seems to inhibit the catalyst redox properties. As a consequence, water and ethanol are not longer activated over these active sites, the catalyst redox cycle is interrupted and finally the catalyst is deactivated.

The Rh inclusion in the CeZrCo oxide prevents the carbonate formation [22]. The ethanol dehydration to produce ethylene is favored at the expense of ethanol dehydrogenation which leads to acetaldehyde production. TPO profiles show that the first oxidation peak, attributed to carbonates species, is small and acetone is not detected in the gas phase. So this catalyst produces less carbonate species and favor the hydrogenation of carbon dioxide (on Rh sites) and/or surface carbon to lead mainly to methane and water, which can be observed by a higher methane percentage in gas phase reaction for CeZrCoRh than for CeZrCo catalyst. Hence, the insertion of Rh in CeZrCo catalyst avoids the accumulation of carbon on the surface. The deactivation still arises after 150 h of steam reforming reaction and the deactivation curve is typical of a deactivation caused by slower blocking sites [13,16]. As a result, the deactivation of the CeZrCoRh after a long period is due to the surface carbon formation, as admitted for hydrocarbons steam reforming, and not principally to carbonates species. Without Rh, acetaldehyde is oxidized into acetate species which decomposes into CO_2, CH_4 and acetone. CO_2 forms surface carbonates which cover the surface of CeZrCo and inhibit water and ethanol activation, leading thus to a rapid deactivation.

5. Conclusions

The insertion of a small amount of noble metal, rhodium, in a ceria-zircon fluorite structure doped with cobalt does not improve the percentage of hydrogen production in gas phase (64.8%), compared to a catalyst free of noble metal (65.1%), but increases by thirty times the lifetime of the metal oxide catalyst.

Rhodium facilitates the reduction of the catalyst even under reactive flow, which increased the reducibility of the catalyst.

Rhodium insertion favors ethylene pathway at the expense of acetaldehyde decomposition way, which creates acetate and carbonates species on the catalyst surface and blocks the active catalyst sites of water and ethanol activation.

References

[1] J.N. Armor, Appl. Catal. A: Gen. 176 (1999) 159.
[2] A. Demirbas, Prog. Energy Combust. Sci. 33 (2007) 1.
[3] M.A. Goula, S.K. Kontou, P.E. Tsiakaras, Appl. Catal. B: Environ. 49 (2004) 135.
[4] J.P. Breen, R. Burch, H.M. Coleman, Appl. Catal. B: Environ. 39 (2002) 65.
[5] C. Diagne, H. Idriss, A. Kiennemann, Catal. Commun. 3 (2002) 565.
[6] J. Rasko, A. Hancz, A. Erdohelyi, Appl. Catal. A: Gen. 269 (2004) 13.
[7] T. Montini, L. De Rogatis, V. Gombac, P. Fornasiero, M. Graziani, Appl. Catal. B: Environ. 71 (2007) 125.
[8] J. Comas, Chem. Eng. J. 98 (2004) 61.
[9] J. Llorca, N. Homs, J. Sales, P. Ramírez de la Piscina, J. Catal. 209 (2002) 306.
[10] F. Aupretre, C. Descorme, D. Duprez, Catal. Commun. 3 (2002) 263.
[11] M.S. Batista, R.K.S. Santos, E.M. Assaf, J.M. Assaf, E.A. Ticianelli, J. Power Sources 124 (2003) 99.
[12] M. Benito, J.L. Sanz, R. Isabel, R. Padilla, R. Arjona, L. Daza, J. Power Sources 151 (2005) 11.
[13] J.C. Vargas, S. Libs, A.C. Roger, A. Kiennemann, Catal. Today 107–108 (2005) 417.
[14] J.C. Vargas, A.C. Roger, A. Kiennemann, Chem. Eng. Trans. 4 (2004) 247.
[15] F. Aupretre, C. Descorme, D. Duprez, Top. Catal. 30–31 (2004) 487.
[16] C.H. Bartholemew, Appl. Catal. A: Gen. 212 (2001) 17.
[17] F. Romero-Sarria, J.C. Vargas, A.C. Roger, A. Kiennemann, Catal. Today 133–135 (2008) 149.
[18] F. Sadi, D. Duprez, F. Gérard, A. Miloudi, J. Catal. 213 (2003) 226.
[19] G. Jacobs, R.A. Keogh, B.H. Davis, J. Catal. 245 (2007) 326.
[20] M. Ni, D.Y.C. Leung, M.K.H. Leung, Int. J. Hydrogen Energy 32 (2007) 3238.
[21] C. Verrier, PhD Thesis, University of Caen, 2006.
[22] H. Idriss, E.G. Seebauer, J. Mol. Catal. A: Chem. 152 (2000) 201.
[23] G.A.M. Hussein, A.K.H. Nohman, K.M.A. Attyia, J. Therm. Anal. Calorim. 42 (1994) 1155.
[24] C. Padeste, N.W. Cant, D.L. Trimm, Catal. Lett. 24 (1994) 95.